Supplementary Figure 1

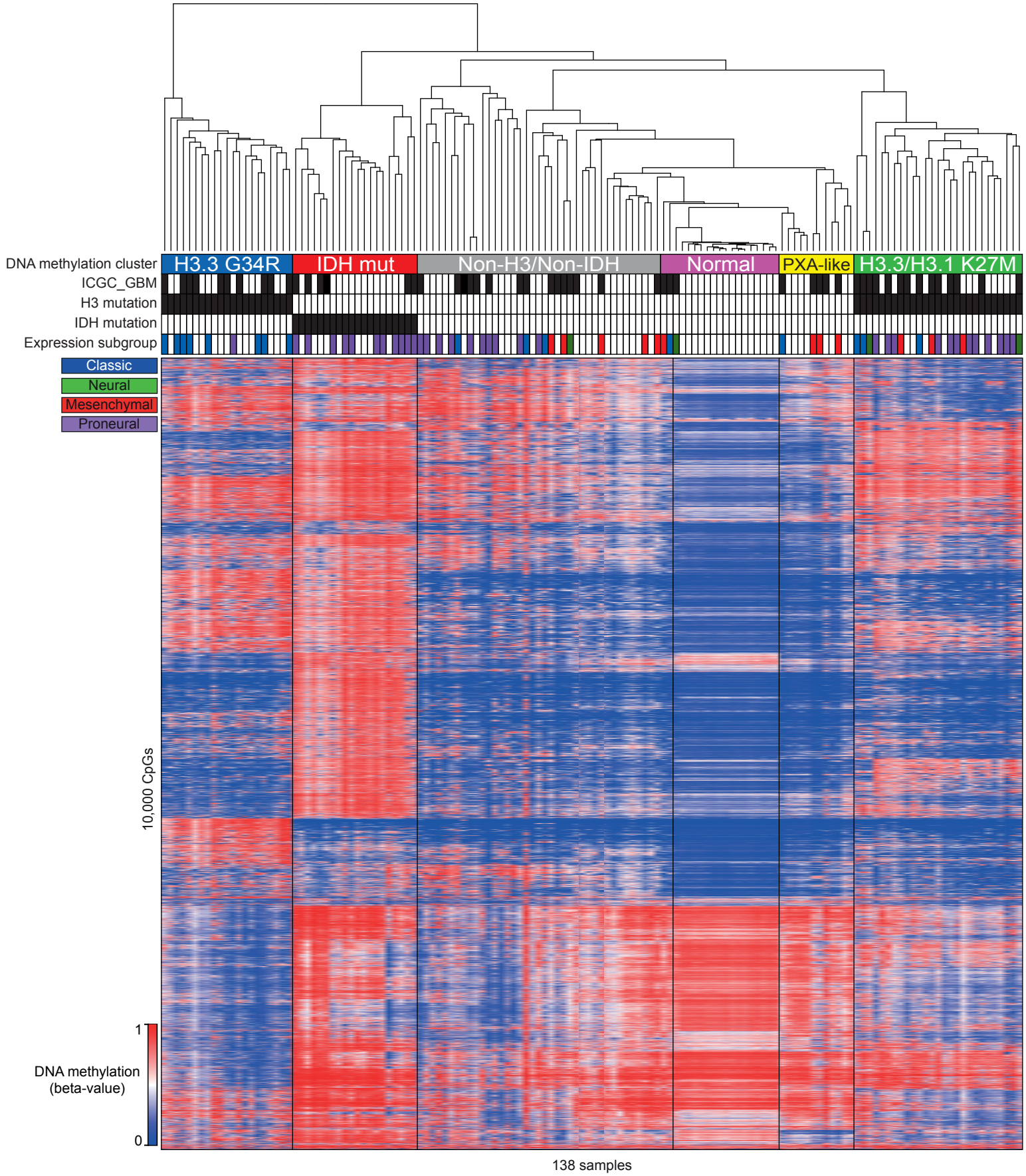

Supplementary Figure 1. Epigenetic pedGBM subgroups.
Heatmap of DNA methylation levels in 122 tumour and 16 normal brain samples generated by unsupervised hierarchical clustering. Each row represents a CpG site, each column represents a sample. The level of DNA methylation (beta-value) is represented with a colour scale as depicted. ICGC_GBMs, histone H3- and IDH-mutant tumours as well as gene expression subgroup association are indicated (where available).

Supplementary Figure 2

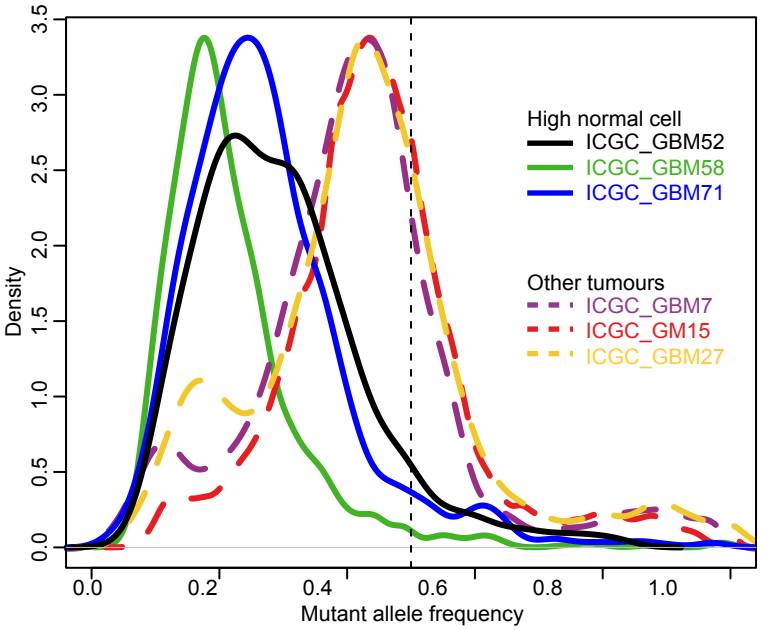

Supplementary Figure 2. Mutant allele frequency in pedGBMs with high normal cell content.
Density plots depicting mutant allele frequency in three pedGBMs with high normal cell content. Mutation frequency distributions of three pedGBMs with purer tumour cell content are shown as a control (dotted lines).

Supplementary Figure 3

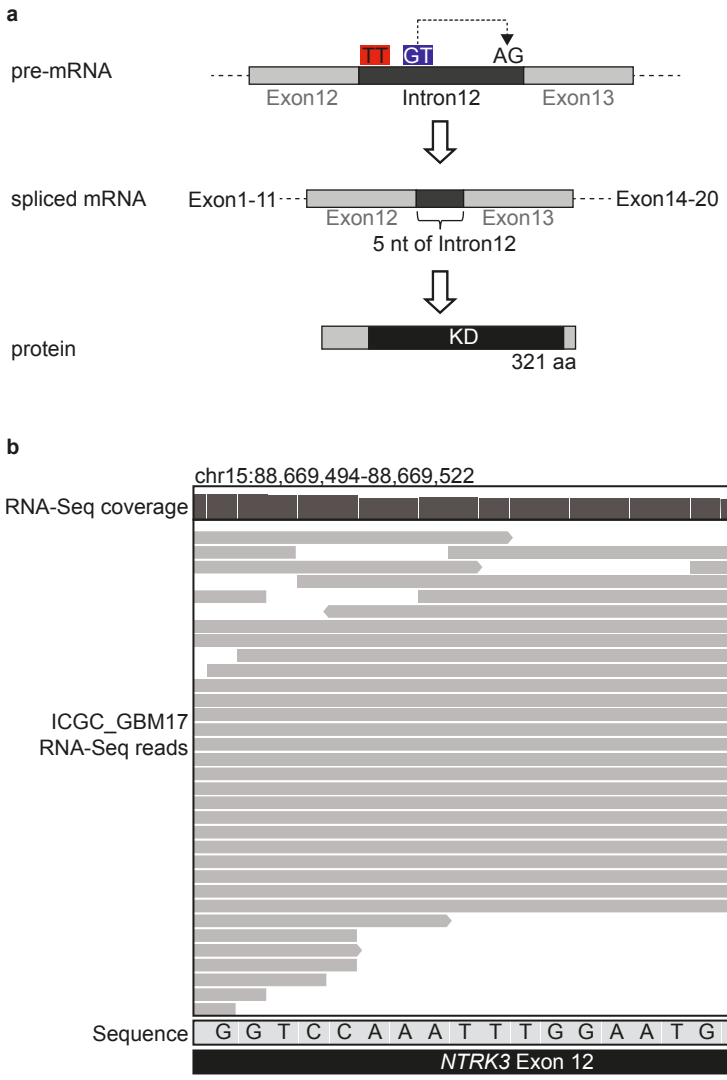

Supplementary Figure 3. *NTRK3* splice site mutation.
a. Effects of the heterozygous splice site mutation within intron 12 of the *NTRK3* gene identified in ICGC_GBM17. Mutation of the regular splice donor site (GT>TT; red) within intron 12 of *NTRK3* results in an alternative transcript, retaining 5 additional nucleotides of intron 12 by using an alternative splice donor (GT; blue). The resulting spliced mRNA encodes an amino-terminally truncated protein containing the NTRK3 kinase domain (KD). **b.** RNA sequencing data of ICGC_GBM17 covering exon 12 of *NTRK3*. While the majority of RNA sequencing reads indicate normal splicing using the regular splice donor (GT; red), several RNA sequencing reads support the splice site mutation (TT; red) and the use of an alternative splice donor (GT; blue) within intron 12 of the *NTRK3* gene.

Supplementary Figure 4

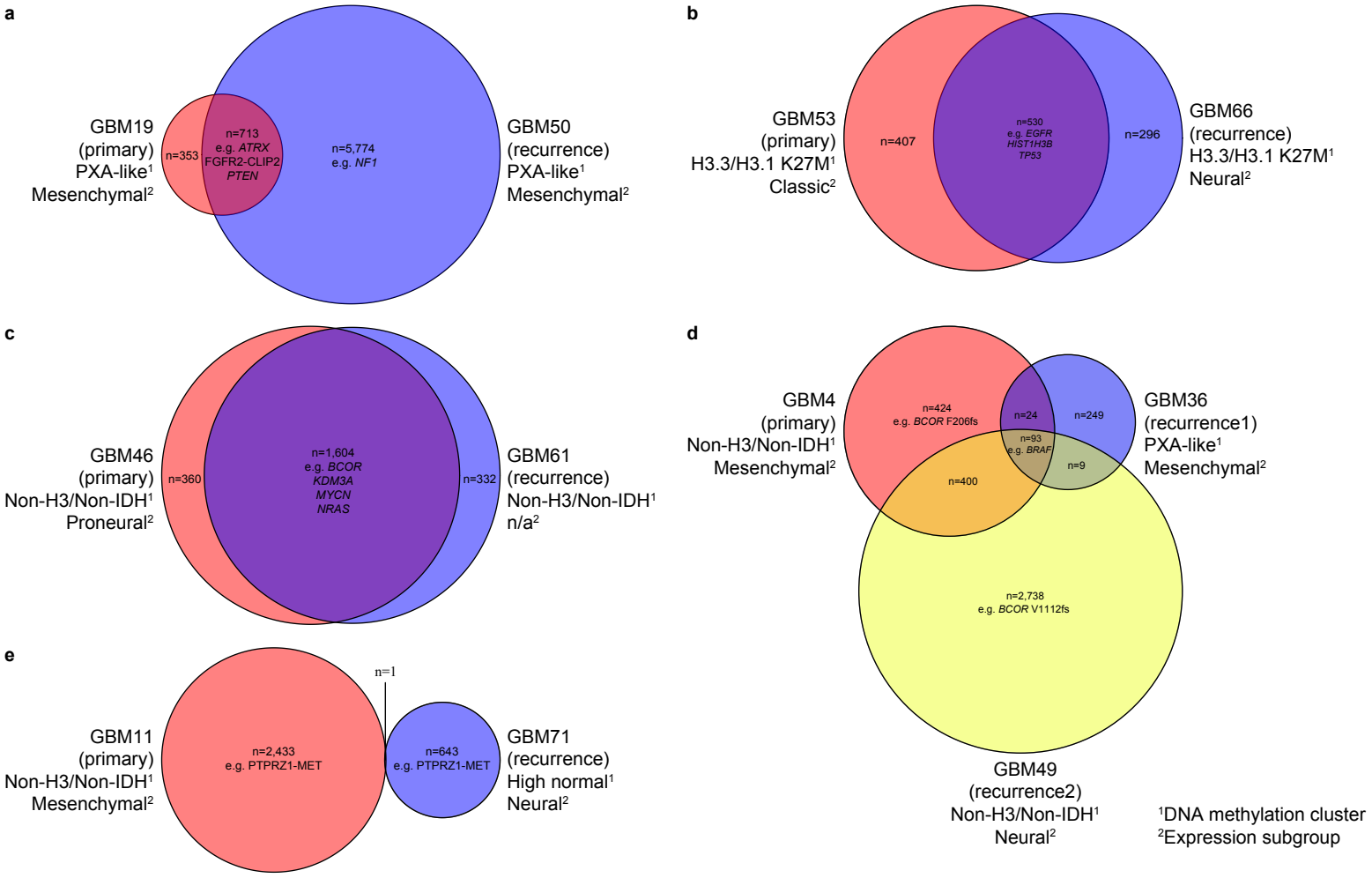

Supplementary Figure 4. Genetic aberrations in pairs of primary and recurrent tumours.
Venn diagrams illustrating overlapping genetic aberrations in 5 pairs of primary and recurrent tumour samples. Overlapping events in glioma-associated genes are listed. DNA methylation as well as gene expression subgroup of tumours is provided if available (n/a: not analysed).

Supplementary Figure 5

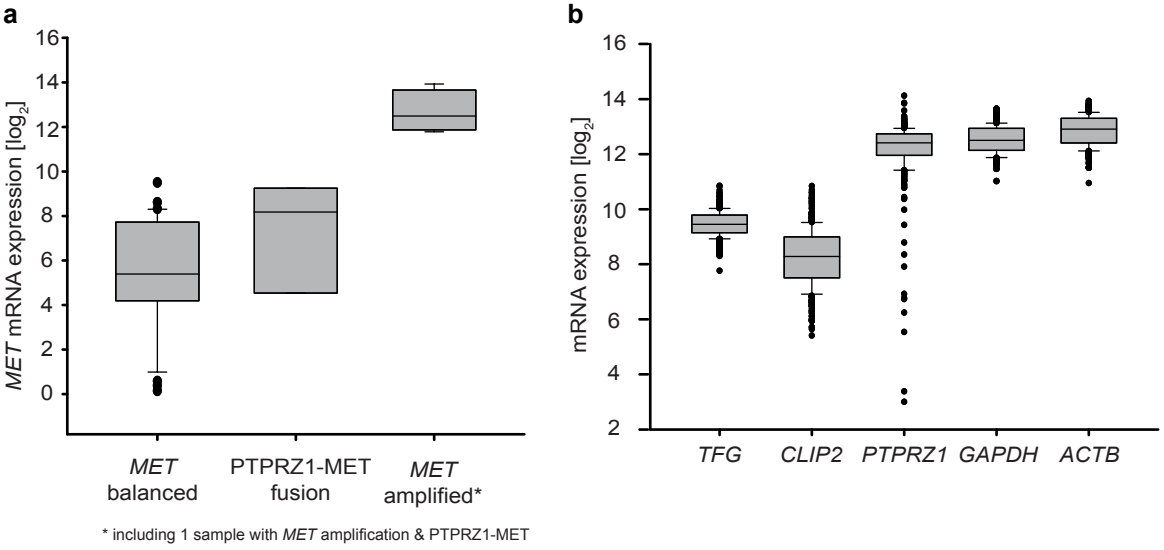

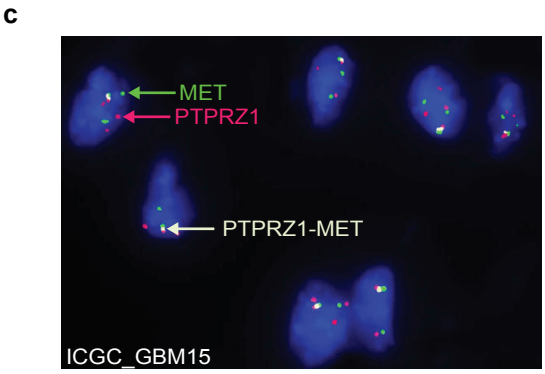

Supplementary Figure 5. Glioblastoma expression and fluorescence *in situ* hybridization data.
a. Scatter plot illustrating *MET* mRNA expression (log_2) of 31 primary pedGBMs with balanced *MET* locus, 4 *MET* amplified tumours (including ICGC_GBM43 with additional PTPRZ1-MET fusion) as well as three PTPRZ1-MET-bearing tumours (ICGC_GBM11, 15 and 71). **b.** Box plot illustrating *TFG*, *CLIP2*, *PTPRZ1*, *GAPDH* and *ACTB* mRNA expression (log_2) in 458 human glioblastomas. **c.** Detection of the PTPRZ1-MET fusion in interphase cell nuclei of ICGC_GBM15 by dual-colour interphase FISH using a PTPRZ1 (red) and MET (green) specific probe.

Supplementary Figure 6

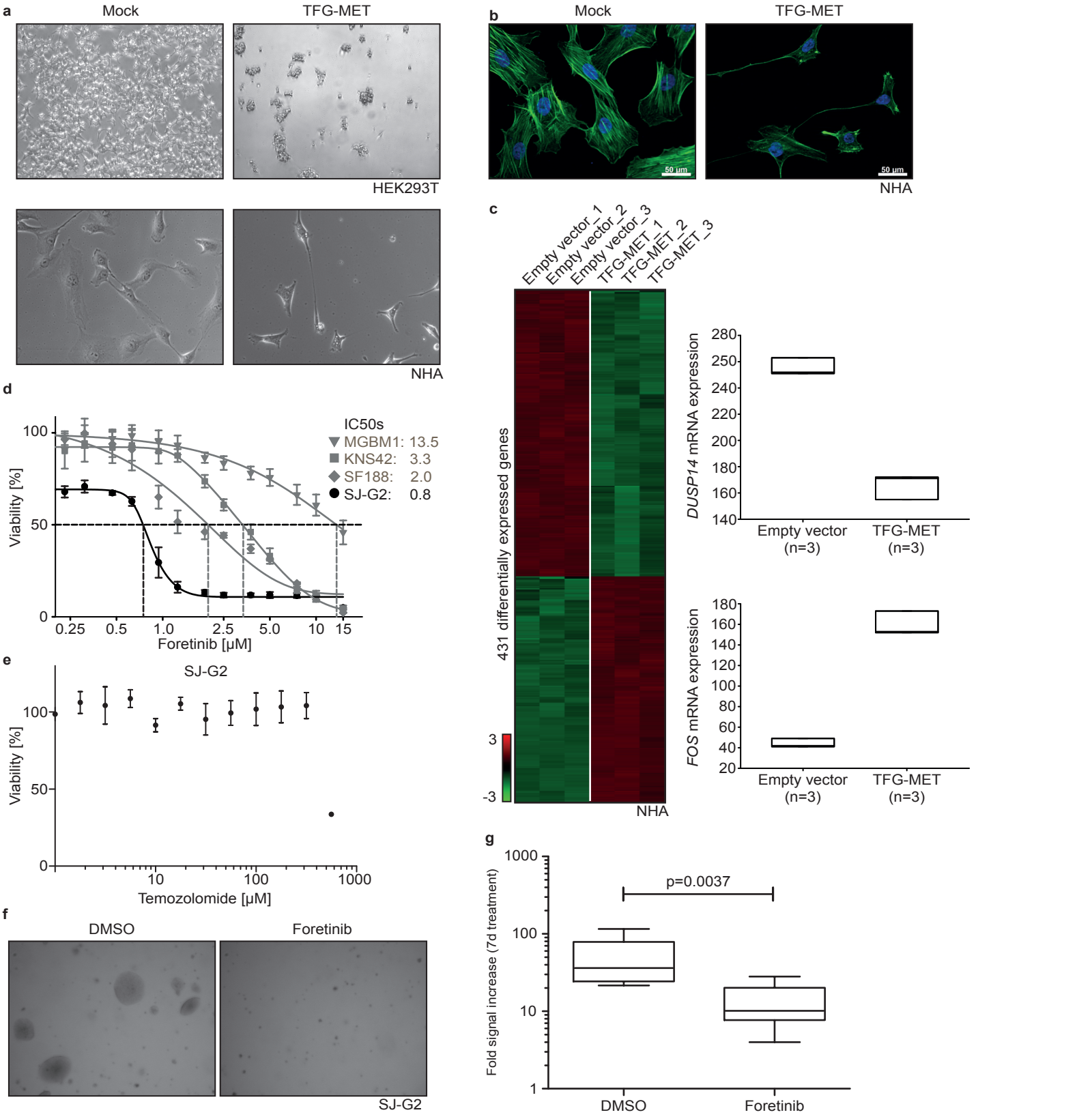

Supplementary Figure 6. MET fusions are sensitive to pharmacological MET inhibitors.
a. Both HEK293T and normal human astrocyte (NHA) cells show increased cell rounding and cell detachment upon TFG-MET overexpression (cell viability was not affected). Mock-transfected/empty vector transduced cells are shown as a control. **b.** Immunofluroescence staining of NHA cells (EV or TFG-MET transduced) for F-actin (phalloidin) indicates a dramatic loss of stress fibres upon TFG-MET expression. **c.** Heatmap of 431 differentially expressed genes identified in TFG-MET-over-expressing NHA (compared to empty vector control). Each row represents a gene, each column represents an experiment, performed in triplicate. The level of gene expression (z-score) is represented with a colour scale as depicted. Boxplots show mRNA expression of the two example genes *DUSP14* and *FOS*. **d.** Effect of foretinib treatment on CLIP2-MET-expressing SJ-G2 glioblastoma cells as well as three other pedGBM cell lines without MET fusion (SF188, KNS-42 and MGBM1). Each assay was measured in triplicates. Error bars represent standard deviation. **e.** Effect of temozolomide treatment on CLIP2-MET-expressing SJ-G2 glioblastoma cells. Each assay was measured in triplicates. Error bars represent standard deviation. **f.** Anchorage independent growth of CLIP2-MET-expressing SJ-G2 glioblastoma cells is inhibited in the presence of 0.5µM foretinib (d12). **g.** Box plot illustrating luciferase signal increase as measured by intravital bioluminescence imaging, which indicates proliferation of RCAS-TFG-MET cells. Tumour cell proliferation/tumour growth was significantly decreased by foretinib treatment (over the course of 7 days) compared to DMSO treated controls (log rank test).

Figure 2B: Full Western Blot membranes

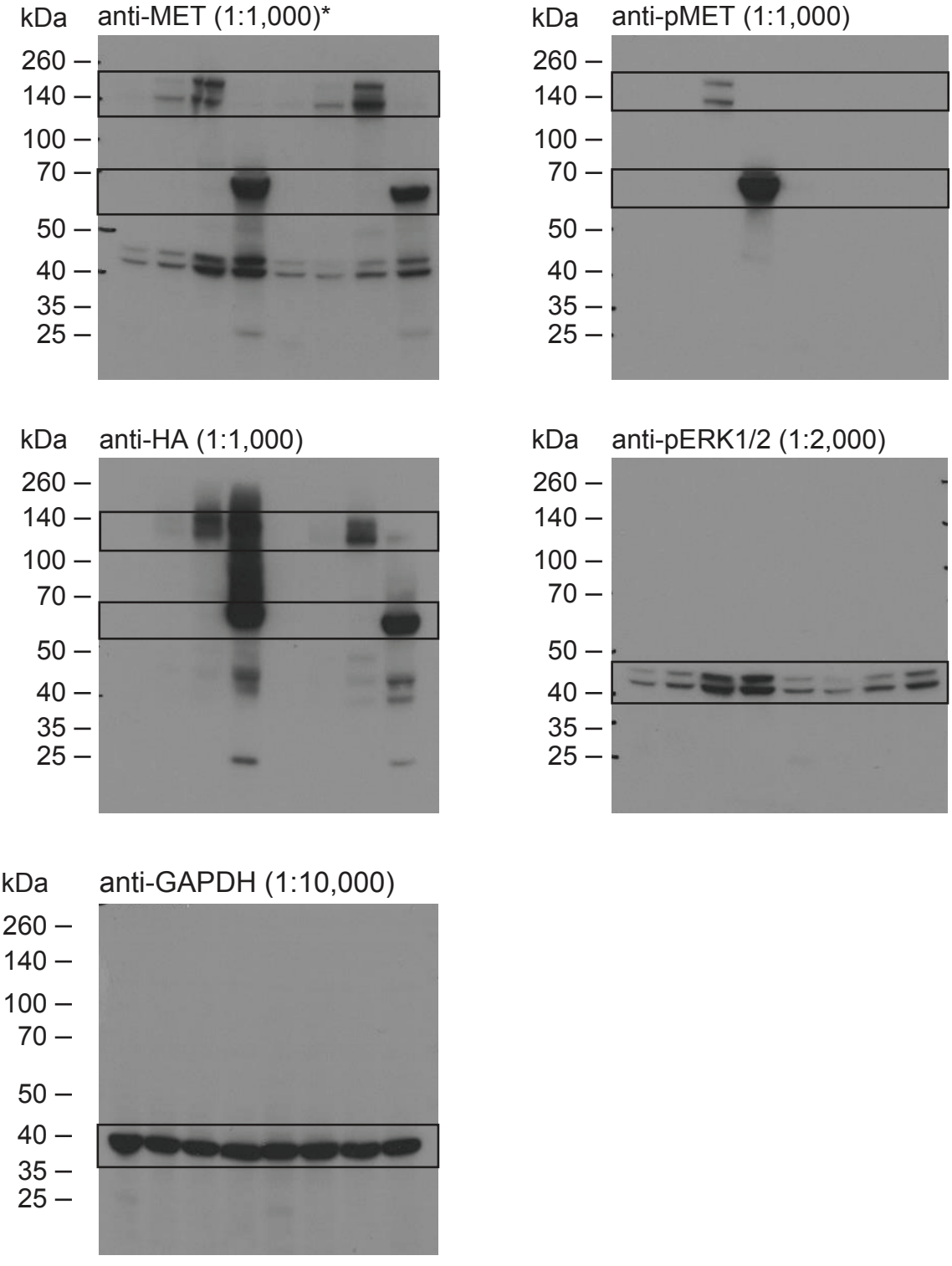

* Western Blot membrane was used to detect pERK1/2 with subsequent reprobing for MET without membrane stripping.

Figure 2C: Full Western Blot membranes

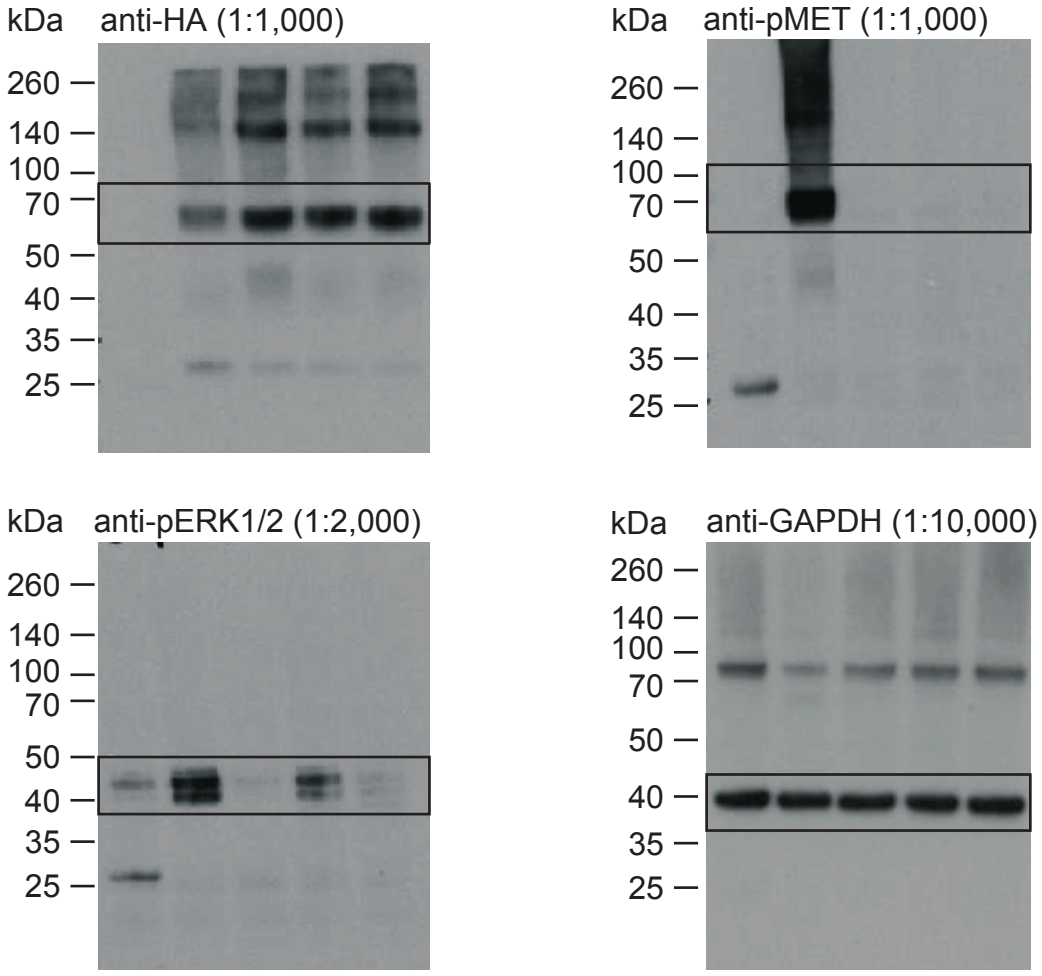

Figure 3G: Full Western Blot membrane

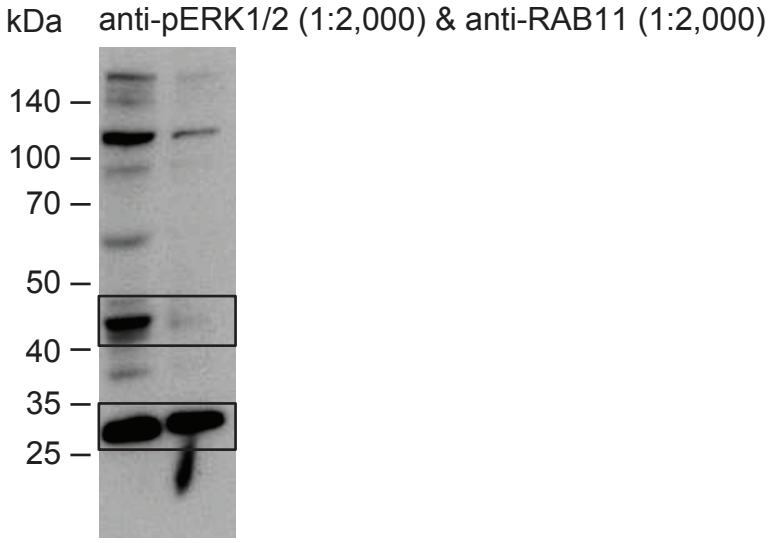

Western Blot membrane was incubated with PathScan Multiplex Western Cocktail I (#5301; Cell Signaling; 1:2,000), which allows simultaneous detection of pERK1/2 and RAB11.